molecules

Article

The Positional Isomeric Effect on the Structural Diversity of Cd(II) Coordination Polymers, Using Flexible Positional Isomeric Ligands Containing Pyridyl, Triazole, and Carboxylate Fragments

Jonathan Cisterna [1], Catherine Araneda [1], Pilar Narea [1], Alejandro Cárdenas [2], Jaime Llanos [3] and Iván Brito [1,*]

[1] Departamento de Química, Facultad de Ciencias Básicas, Universidad de Antofagasta, Casilla 170, Antofagasta 1240000, Chile; jonathan.cisterna@uantof.cl (J.C.); catherine.araneda@gmail.com (C.A.); pilar.narea@uantof.cl (P.N.)

[2] Departamento de Física, Facultad de Ciencias Básicas, Universidad de Antofagasta, Casilla 170, Antofagasta 1240000, Chile; alejandro.cardenas@uantof.cl

[3] Departamento de Química, Universidad Católica del Norte, Av. Angamos 0610, Antofagasta 1240000, Chile; jllanos@ucn.cl

* Correspondence: ivan.brito@uantof.cl; Tel.: +56-55-2637814

Received: 7 September 2018; Accepted: 10 October 2018; Published: 14 October 2018

Abstract: To systematically investigate the influence of the positional isomeric effect on the structures of polymer complexes, we prepared two new polymers containing the two positional isomers ethyl 5-methyl-1-(pyridin-3-yl)-1*H*-1,2,3-triazole-3-carboxylate (**L1**) and ethyl-5-methyl-1-(pyridin-3-yl)-1*H*-1,2,3-triazole-4-carboxylate (**L2**), as well as Cd(II) ions. The structures of the metal–organic frameworks were determined by a single crystal XRD analysis. The compound $[Cd(L1)_2{\cdot}4H_2O]$ (**1**), is a hydrogen bond-induced coordination polymer, whereas the compound $[Cd(L2)_4{\cdot}5H_2O]_n$ (**2**) is a three-dimensional (3-D) coordination polymer. Their structures and properties are tuned by the variable N-donor positions of the ligand isomers. This work indicates that the isomeric effect of the ligand isomers plays an important role in the construction of the Cd(II) complexes. In addition, the thermal and luminescent properties are reported in detail.

Keywords: metal-organic frameworks; Cd(II) complexes; X-ray diffraction analysis; thermal properties; luminescence

1. Introduction

The self-assembly of coordination polymers and metal–organic frameworks (MOFs) [1–3] has been attracting great attention in the past decade, mainly because of their great potential as functional materials for diverse technological applications [4–8]. In particular, the luminescent properties of this type of material, as well as the possibility of fine-tuning the characteristics of their emission by carefully selecting both the metal and the organic ligands, have been a topic of special relevance in this field [9–13].

In this sense, the well-studied luminescent properties [14–18] of d^{10} cations, such as Cu(I), Ag(I), and Au(I), as well as their versatility in the construction of complex coordination networks with different types of organic ligands have been the object of interest.

From a structural point of view, the two principal themes in this field have been the synthesis of compounds that have either discrete molecular architectures with polyhedral or polygonal shapes or infinite coordination polymers in one, two, or three dimensions (1-D, 2-D, or 3-D, respectively) composed of metal ions in combination with deliberately tailored organic ligands. In the latter case, the resulting network topology [19] for the supramolecular complex can usually be predicted by selecting the chemical structure of the organic ligands and the usual coordination geometry of the metal ions linking the ligands together in the final structure [20]. The structural properties of the bridging ligands, such as their rigidity or flexibility, length, size, bulkiness, and linear or nonlinear geometry, have been found to play an important role in the construction of specific macromolecular architectures [21–23].

One crucial aim of this work is to explore the essential factors of positional isomeric ligands for regulating the structural assembly of Cd(II) MOFs, which may provide further insight into the design of new functional crystalline materials [24–28].

2. Materials and Methods

2.1. Reagents and Instruments

All chemicals were of A.R. grade and used without further purification (Sigma-Aldrich, St. Louis, MO, United States). FT-IR spectra in the range of 400–4000 cm^{-1} were obtained, using KBr pellets, with a Nicolet Avatar 330 spectrometer (Thermo Scientific, Waltman, MA, United States). The elemental analyses were obtained on a CNHS FLASH EA 1112 Elemental analyzer (Thermo Scientific, Waltman, MA, United States). HR-ESI-MS were obtained on a Waters (Micromass) AutoSpec mass spectrometer (Water co.; Milford, MA, United States). Powder X-ray diffraction data were obtained on a Bruker D8 Advance diffractometer (Cu-Kα radiation (λ = 0.1542 nm); Bruker Co.; Billerica, MA, United States). The thermogravimetric analyses were carried out in an N_2 atmosphere on a Mettler Toledo DL31 thermoanalyzer (Mettler Toledo enterprise, Columbus, OH, United States) with a heating rate of 10 °C/min. The luminescence spectra were recorded on a JASCO FP-8500 spectrofluorometer (JASCO Co.; Kyoto, Japan). The excitation was performed with λ_{ex} = 360–370 nm, and the emission was recorded at λ_{em} = 410–450 nm.

2.2. Single-Crystal X-ray Diffraction

The diffraction data for compound **1** were collected on an automated D8 Venture Bruker diffractometer (Bruker Co.; Billerica, MA, United States) equipped with a two-dimensional CMOS detector (graphite monochromator, λ(MoKα) = 0.71073 Å, ω-scans). For compound **2**, λ(CuKα) = 1.5418 Å radiation (ω-scans) was used. Integration, absorption, correction, and determination of unit cell parameters were performed using the APEX3 program package [29]. The structures were solved by a dual space algorithm (SHELXT [30]) and refined by the full-matrix least squares technique (SHELXL [31]) in the anisotropic approximation (except hydrogen atoms). The final formula of compound **2** was calculated from the data of the PLATON/SQUEEZE procedure [32] (196 ē in 699 Å^3, equivalent to around 10 disordered ethanol molecules). Additional crystallographic details are available in the CIF files. ORTEP views were drawn using OLEX^2 software (version 1.12, Olexsys Ltd., Durham University, Durham, UK) [33]. The crystallographic data and details of the structure refinements are summarized in Table 1. CCDC 1515697 (**L1H**), 1515698 (**L2H**), 1866538 (**1**), and 1866353 (**2**) contain the supplementary crystallographic data for this paper. These data can be obtained free of charge from the Cambridge Crystallographic Data Center at http://www.ccdc.cam.ac.uk/data_request/cif.

Table 1. Crystal data parameters for compounds **L1H**, **L2H**, **1**, and **2**.

Compound	L1H	L2H	1	2
Empirical Formula	$C_9H_8N_4O_2$	$C_9H_8N_4O_2$	$C_{18}H_{22}CdN_8O_8$	$[C_{18}H_{14}CdN_8O_4]_n$
Formula mass, g·mol^{-1}	204.19	204.19	590.84	518.77
Collection T, K	295.21	296.27	295.51	297.22
crystal system	orthorhombic	Monoclinic	Monoclinic	Monoclinic
space group	$Pna2_1$	Cc	$P2_1/c$	$P2_1/n$
a (Å)	13.4617(12)	18.5248(10)	9.9864(5)	10.7368(8)
b (Å)	3.7613(3)	3.7425(2)	7.3650(4)	14.8147(14)
c (Å)	17.9448(16)	13.0186(7)	15.7758(9)	15.7859(14)
α (°)	90	90	90	90
β (°)	90	92.154(4)	104.846(3)	99.017(3)
γ (°)	90	90	90	90
V (Å^3)	908.61(14)	901.93(8)	1121.57(11)	2479.9(4)
Z	4	4	2	4
ρ_{calcd} (g·cm^{-3})	14.926	1.504	1.750	1.389
Crystal size (mm)	0.402 × 0.24 × 0.108	0.414 × 0.129 × 0.114	0.13 × 0.102 × 0.073	0.459 × 0.433 × 0.258
F(000)	425.5	424.0	596.0	1032.0
abs coeff (mm^{-1})	0.931	0.938	8.372	0.917
θ range (°)	9.86 to 122.94	9.556 to 117.866	9.16 to 118.36	5.5 to 56.75
range h,k,l	−14/15, −4/4, −19/19	−20/20, −4/4, −13/14	−11/11, −8/8, −17/17	−12/14, −1 9/19, −21/21
No. total refl.	13089	8282	24642	52471
No. unique refl.	1328	1242	1598	6169
Comp. θ_{max} (%)	94.0	97.0	98.3	99.4
Max/min transmission	0.765/0.904	0.865/0.899	0.413/0.543	0.663/0.78
Data/Restraints/Parameters	1328/5/138	1242/2/139	1598/0/164	6169/0/282
Final R [$I > 2\sigma(I)$]	R_1 = 0.0490, wR_2 = 0.1363	R_1 = 0.0445, wR_2 = 0.1004	R_1 = 0.0392, wR_2 = 0.0779	R_1 = 0.0415, wR_2 = 0.0922
R indices (all data)	R_1 = 0.0618, wR_2 = 0.1415	R_1 = 0.0557, wR_2 = 0.1077	R_1 = 0.0614, wR_2 = 0.0849	R_1 = 0.0631, wR_2 = 0.1041
Goodness of fit/F^2	1.094	1.124	1.065	1.036
Largest diff. Peak/hole(eÅ^{-3})	0.33/−0.35	0.18/−0.15	0.72/−0.58	1.93/−0.63
Flack Parameter	0.0(5)	0.4(2)	—	—

2.3. Synthetic Procedures

2.3.1. General Procedure for the Syntheses of Ligands **L1** and **L2**

The organic ligands ethyl 5-methyl-1-(pyridin-3-yl)-1*H*-1,2,3-triazole-3-carboxylate (**L1**) and ethyl 5-methyl-1-(pyridin-3-yl)-1*H*-1,2,3-triazole-4-carboxylate (**L2**) were prepared according to standard methods reported in the literature [34], generating the precursor ester compounds. The esters were saponified with a solution of NaOH in order to generate the corresponding carboxylate sodium salts—compounds **L1** and **L2**, respectively.

L1: Yield: quant. IR (KBr, cm^{-1}); ν: 3062, 3036 (CAr-H); 2981 (Csp_3-H); 1630 (C=O-), 1508 (N=N); 1483, 1466, 1447 (CAr-CAr); 1446 (COO-as). ^{1}H-NMR (500 MHz, DMSO) δ (ppm): 8.72 (s, 1H, H5), 8.71 (d, *J* = 1.3 Hz, 1H, H3), 8.02 (d, *J* = 7.2 Hz, 1H, H1), 7.66 (dd, *J* = 7.9, 4.6 Hz, 1H, H2), 2.45 (s, 3H, H12). ^{13}C-NMR (500 MHz, DMSO) δ (ppm): 166.20 (C13), 151.13 (C3), 146.15 (C5), 144.32 (C8), 136.67 (C9), 134.12 (C1), 133.65 (C6), 125.64 (C2), 10.20 (C12). HR-ESI-MS for $C_9H_7N_4O_2Na$ $[M + H]^+$: calculated = 226.2, found = 226.1 (1 ppm).

L2: Yield: quant. IR (KBr, cm^{-1}); ν: 3102, 3055 (CAr-H); 2981 (Csp3-H); 1606 (C=O); 1489 (N=N); 1473, 1446, 1421 (CAr-CAr); 1427 (COO-as). ^{1}H-NMR (500 MHz, DMSO) δ (ppm): 8.77 (dd, *J* = 4.6, 1.5 Hz, 2H, H2, H4), 7.67 (dd, *J* = 4.6, 1.5 Hz, 2H, H1, H5), 2.57 (s, 3H, H12). ^{13}C-NMR (500 MHz, DMSO) δ (ppm): 166.11 (C13), 151.97 (C2, C4), 144.46 (C6), 143.61 (C8), 136.20 (C9), 119.54 (C1, C5), 10.40 (C12). HR-ESI-MS for $C_9H_7N_4O_2Na$ $[M + H]^+$: calculated = 226.2, found = 226.0 (2 ppm).

2.3.2. Synthesis of Tetraaqua–bis(5-methyl-1-(3-pyridin)-1*H*-1,2,3-triazole-carboxilate) Cadmium(II) $[Cd(L1)_2 \cdot 4H_2O]$ (**1**)

A solution of **L1** (10 mg, 0.0442 mmol) in H_2O (5 mL) was added to a solution of $Cd(NO_3)_2 \cdot 4H_2O$ (6.28 mg, 0.0221 mmol) in *n*-butanol (5 mL). The resulting clear solution was kept at room temperature for 30 days until the crystals formed. The colorless crystals of compound **1** were filtered, washed with dimethylformamide (DMF), and dried in air. The yield was 0.0084 g (70%).

2.3.3. Synthesis of Catena-tetra(5-methyl-1-(4-pyridin)-1*H*-1,2,3-triazole-carboxilate) Cadmium(II) Pentahydrate $[Cd(L2)_4]_n$ (**2**)

A solution of **L2** (10 mg, 0.0442 mmol) in H_2O (5 mL) was added a solution of $Cd(NO_3)_2{\cdot}4H_2O$ (6.28 mg, 0.0221 mmol) in ethanol (5 mL). The mixture was homogenized in an ultrasonic bath at 60 °C for 40 min, and then placed in a Teflon-lined stainless steel vessel, heated to 120 °C for three days, and cooled to room temperature over 24 h. Colorless needle crystals of compound **2** were obtained. The yield was 0.0063 g (60%).

3. Results

3.1. *Syntheses of* **L1** *and* **L2**

The syntheses of both compounds were carried out according to the literature [34,35], using [3 + 2] dipolar cycloaddition between *n*-pyridyl azide (*n* = 3 or 4) and a 1,3-dicarbonyl compound such as ethyl acetoacetate (see Scheme 1). In general, the yields of the ester precursors are in the range of 35-70% and the yields of the sodium carboxylate salts **L1** and **L2** are quantitative.

The obtained compounds were hygroscopic, and consequently had to be stored in a dry box or under an in inert gas atmosphere. On the other hand, the ligand **L1** and **L2** are stable under atmospheric conditions. Both are white powders that are soluble in water and other protonic solvents, such ethanol or hot methanol.

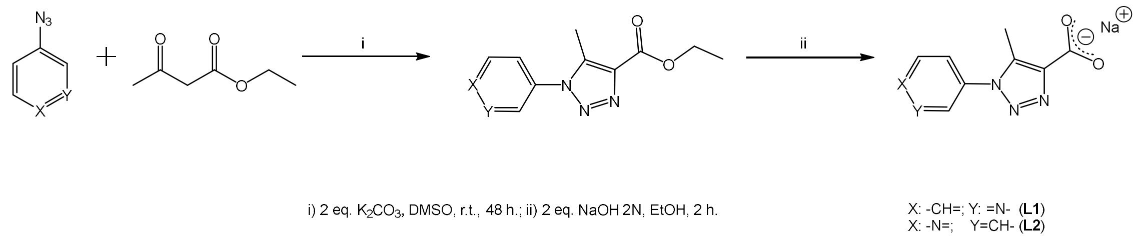

Scheme 1. General synthetic route of ligand **L1** and **L2**.

Finally, suitable single crystals for XRD analysis were isolated. The crystal structure data reveal that both compounds crystallize in their protonic forms (see Section 3.2)

3.2. *Syntheses of* **1** *and* **2**

The Cd(II) compounds were obtained using immiscible liquid for ion diffusion, generating single crystals in the interphase. In the case of $[Cd(L1)_2{\cdot}4H_2O]$ (**1**), the single crystals were manually isolated out of the reaction mixture of $Cd(NO_3)_2{\cdot}4H_2O$ and **L1** in a mixture of 1:1 H_2O and *n*-butanol. In the same way, the synthesis of $[C_{18}H_{14}CdN_8O_4]_n$ compound **2**, gave rise to suitable crystals from the reaction mixture of $Cd(NO_3)_2{\cdot}4H_2O$ and **L2** in a mixture of 1:1 H_2O/ethanol. The stoichiometric ratio between Cd(II) salt and **L1** or **L2** was 1:2, respectively (see Section 2.3 for more details). Both compounds generated clear colorless single crystals for XRD analyses. In particular, for compound **2**, it was synthesized via solvothermal methods. According to the structural nature of these ligands, compound **1** generated a discrete coordination compound. Meanwhile, compound **2** generated a coordination polymer's 3D architecture (see Scheme 2 and Section 3.3 for more details.).

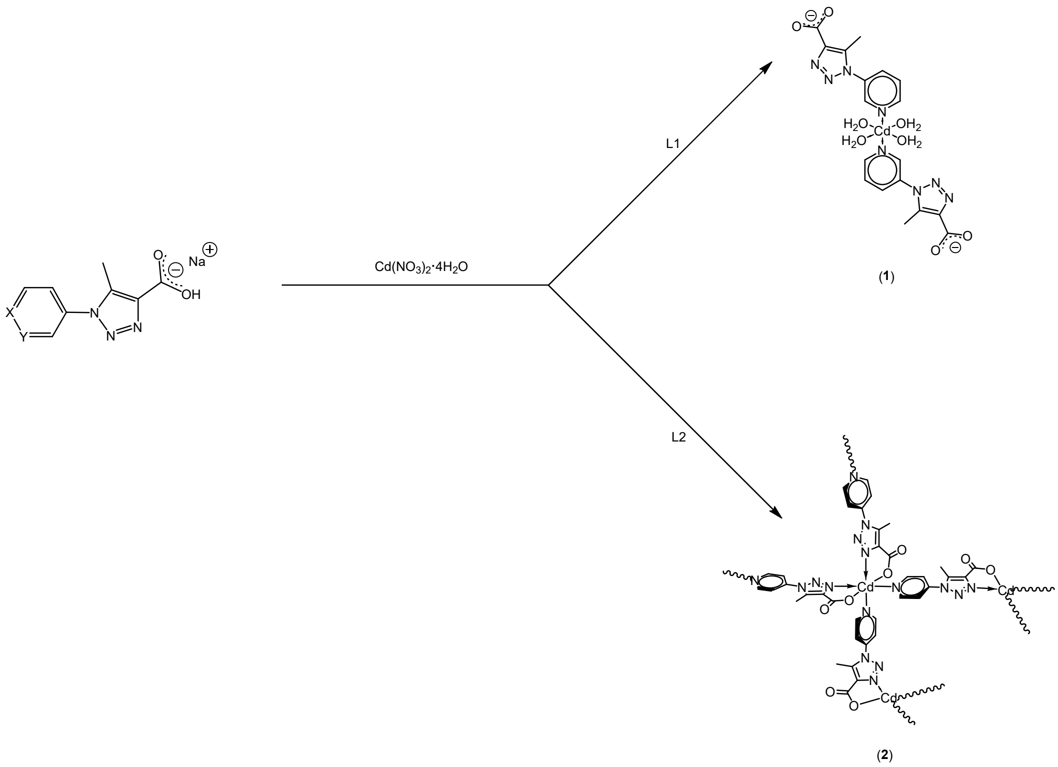

Scheme 2. General synthetic route of compounds **1** and **2**.

3.3. Crystallographic Studies

The crystal structures and chemical compositions of all compounds were established by the single-crystal X-ray diffraction method. The molecular structures of **L1** and **L2** show their protonated forms **L1H** and **L2H** (see Figure 1), corresponding to their respective carboxylic acids. **L1H** crystallizes in the orthorhombic system with space group P*na*2_1, and **L2H** crystallizes in a monoclinic system with space group *Cc*, both compounds with four molecular entities per unit cell with non-centrosymmetric settings. All the distances and angles are normal. The bond lengths between single and double bonds are typical for these types of compounds [36]. It can observed that there is a loss of coplanarity between the respective heterocycles (*n*-pyridyl and 1,4-disubstituted-1,2,3-1*H*-triazole moieties), where the torsion angle between their heterocycles is lower in **L2H** than in **L1H** with 36.8(5) and 39.1(8)°, respectively, following the same tendency in similar compounds previously reported with the same moieties [34,37].

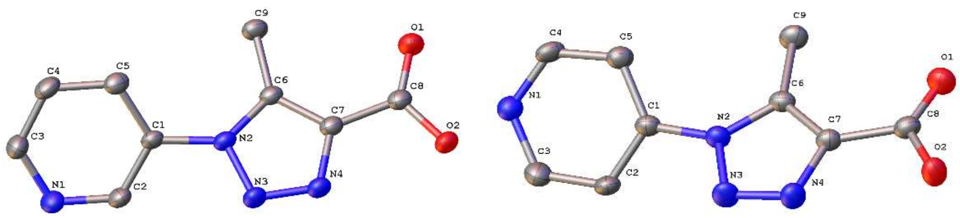

Figure 1. ORTEP plot for compounds **L1H** (**left**) and **L2H** (**right**). Hydrogen atoms were omitted for clarity's sake. Thermal ellipsoids were drawn with 30% of probability.

The crystal structures of both compounds show hydrogen bonding interactions generated with -O(2)-H(2)···N(1), generating slabs along the (101) plane with graph set $C_1^1(9)$ in the crystal packing (see Figure 2). This situation has been reported before in compounds with similar features [37,38].

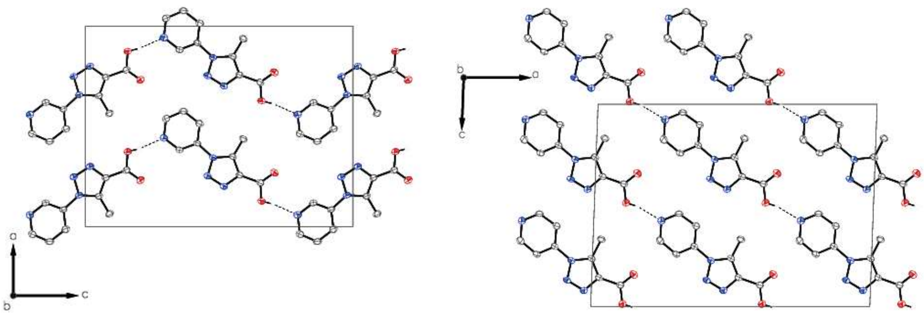

Figure 2. Crystal packing of compound **L1H** (**left**) and **L2H** (**right**).

In compound **1**, the asymmetric unit contains a Cd(II) cation, two water molecules, and two molecules of **L1**. The Cd(II) ion lies on an inversion center and is hexacoordinate with a $[N_2O_4]$ coordination sphere (four water molecules and two N donor atoms from the pyridyl moiety of **L1**) in a distorted octahedral geometry (see Figure 3). The bond lengths and angles around the Cd(II) ion are in the range of 2.280(3)–2.294(3) Å for Cd-O, and 2.358(4) Å for Cd-N. The angles O-Cd-O and O-Cd-N are 86.57(13)-180.0° and 88.59(14)-91.41(14)°, respectively. These bond lengths and angles are similar to the reported values of related Cd(II) complexes containing carboxylate and pyridyl fragments [39,40]. Compound **1** exhibits parallel packing, generating a slab along the (101) plane (see Figure 4). Moreover, an induced hydrogen bond framework in the whole cell generates a spiral shape, due to the 2_1-screw axis and perpendicular glide plane. The hydrogen bonding interactions along the slab are located between water molecules in the equatorial positions of the coordination core and carboxylate fragments, specifically the O(3) and O(4) atoms.

The coordinated water molecules and the carboxylate groups are involved in the formation of a two-dimensional hydrogen-bonded network, which consolidates the crystal packing (see Figure 4).

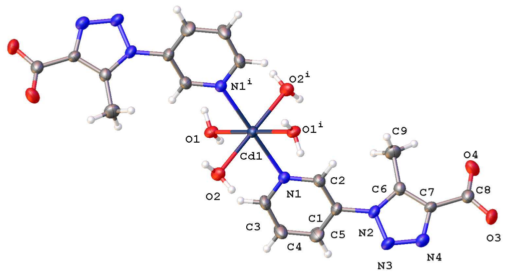

Figure 3. View of local coordination geometry at the Cd(II) center in compound **1** (30% ellipsoid probability). Symmetry code (i) is 1 − x,1/2 + y,3/2 − z.

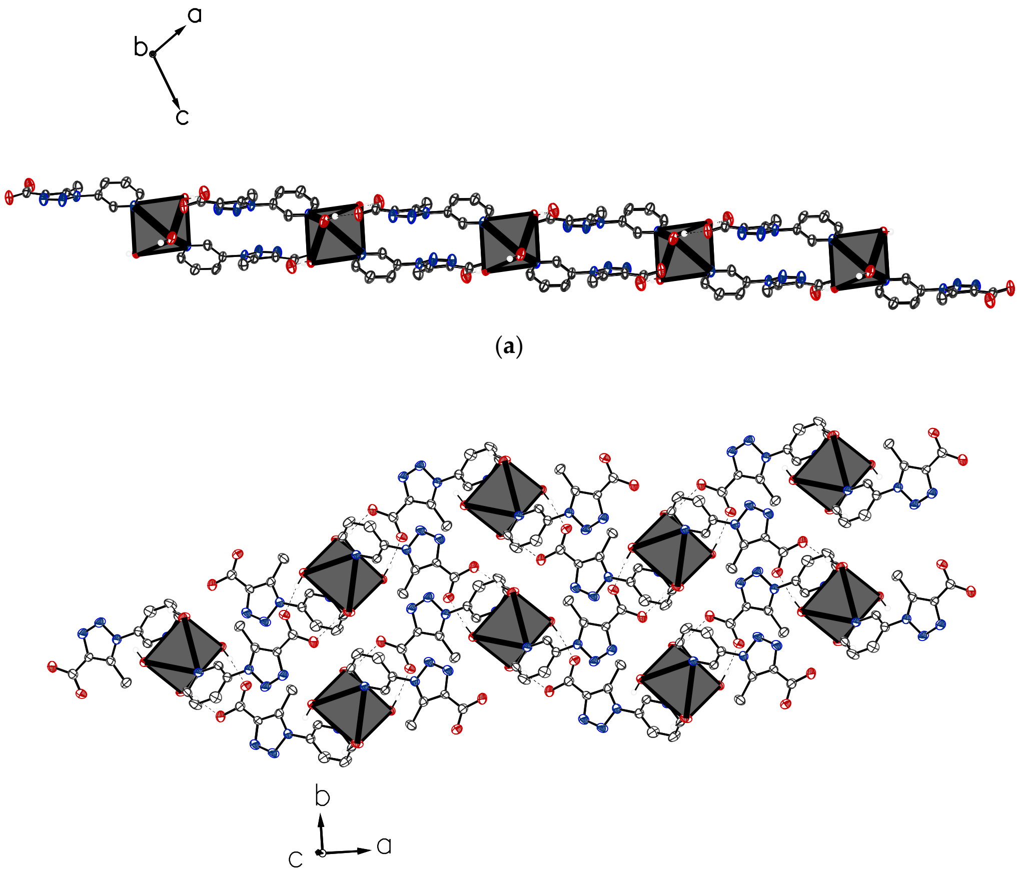

(**a**)

(**b**)

Figure 4. Slabs generated along the (101) plane (**a**) and the (110) plane (**b**), showing the coordination polyhedral.

The crystal structure and chemical composition of compound **2** were established by the single-crystal X-ray diffraction method. The asymmetric unit of compound **2** contains a Cd(II) cation, the coordination environment of which consists of two N atoms of the pyridine, as well as triazole fragments and one O atom of the carboxylate group from two ethyl 5-methyl-1-(pyridin-4-yl)-1*H*-1,2,3-triazole-3-carboxylate ligands **L2** (Figure 5). In the symmetry-unique part of the molecule, the pyridine and chelate ring (N4/C6/C9/O2/Cd1) form a dihedral angle of 89.5(3).

The Cd(II) ion is coordinated in a slightly distorted octahedral geometry by four N atoms and two O atoms from the ethyl 5-methyl-1-(pyridin-4-yl)-1*H*-1,2,3-triazole-3-carboxylate ligands, (Figure 6). The Cd-O distances range from 2.278(3)–2.296(3) Å, and the Cd-N distances range from 2.291(3)–2.348(3) Å. The O-Cd-O angle is 94.64(11)°, and the O-Cd-N and N-Cd-N angles are in the range of 71.41(10)–166.39(10 and 89.38(11)−154.39(11)°, respectively. The Cd–O (carboxylate) and Cd–N bond parameters are in agreement with related Cd(II) complexes containing carboxylate and pyridyl fragments [39,40]. The mean plane defined by pyridine rings (N1/C1/C2/C3/C4/C5 and N5/C10/C11/C12/C13/C14 for plane 1 and plane 2, respectively) makes an angle of 123.81(14)°, and the chelate mean plane defined by Cd1/N8/C15/C18/O3 and Cd1/N4/C6/C9/O2 (plane 3 and plane 4, respectively) makes an angle of 89.00(10)°.

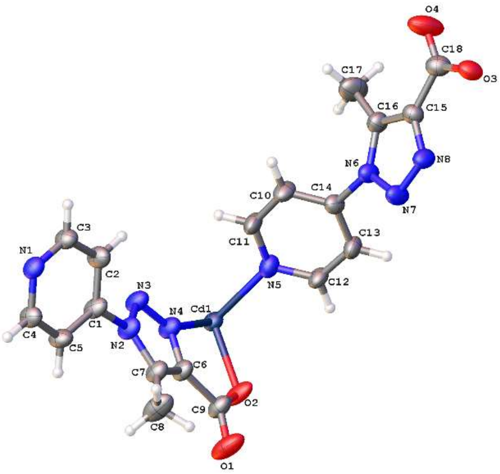

Figure 5. The asymmetric unit of compound **2**.

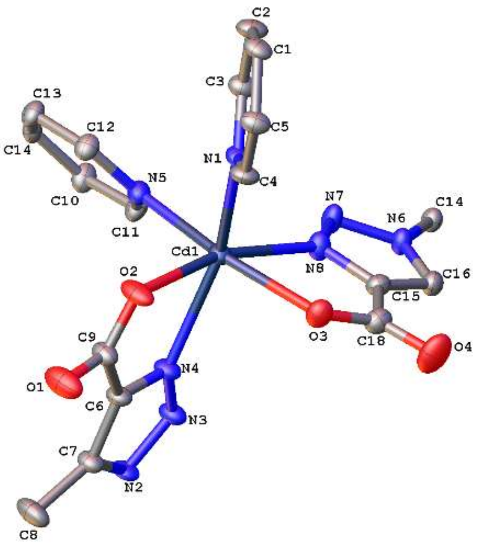

Figure 6. Coordination environment of [Cd(L2)]n cores.

The main structural comparison between compounds **1** and **2** shows the isomeric positional effect in the ligand, because the ligands of compound **1** generate discrete molecular systems, while its positional isomer ligand 2, generates 3D metal–organic frameworks (see Figure 7).

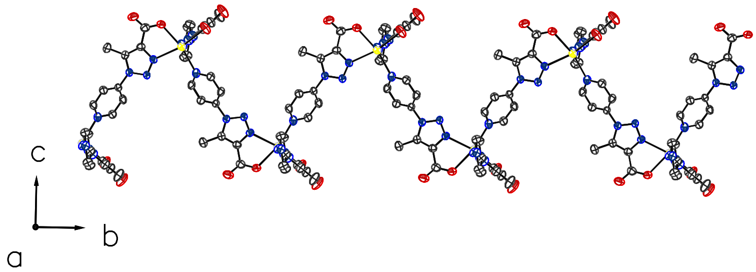

(**a**)

Figure 7. *Cont*.

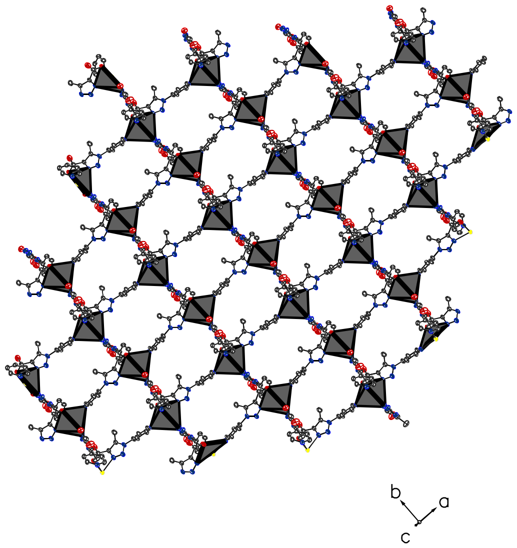

(**b**)

Figure 7. Three-dimensional (3-D) metalorganic frameworks along to plane (100) (**a**) and the plane (111) (**b**).

Another structural consequence of the isomeric effect is the generation of voids within the MOF material, which have a rhombohedral shape with a volume of 1337 Å^3. These voids make this MOF a good candidate as a storage material or luminescent sensor, due to the ability to catch small molecules within in the voids (see Figure 8).

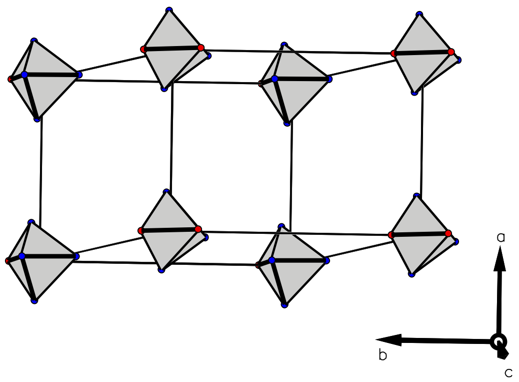

Figure 8. Supramolecular Boxes.

3.4. Thermal Stability Studies

The TGA of both compounds were recorded with a heating rate of β = 10 °C·min^{-1} under a dynamic nitrogen atmosphere in the temperature interval of 20–1000 °C. All curves are shifted to a higher temperature at constant heating rate. The TG curves show a five-step weight loss until total decomposition. Compound **1** shows a decomposition starting at ca. 60 °C, with total decomposition over 600 °C. The first step corresponds to around two H_2O molecules, due to moisture present in the sample (~6%). In the second step at ~150°C, the weight loss of water ligand molecule was ~3%. Over 300 °C, the decarboxylation from the ligand was founded (~8%). The two following steps correspond to progressive decomposition of the compound **1**. The TG curve of compound **2** shows a two-step decomposition curve. The first one at 186 °C represents a weight loss of 5% (two water molecules). The second step at ca. 290 °C corresponds to progressive decomposition of the organic ligand. The final compound after total decomposition of product **2** corresponds to cadmium oxide. (Figure 9).

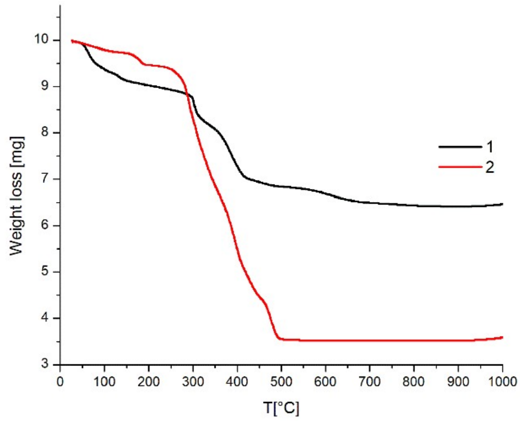

Figure 9. TGA plot of compounds **1** and **2**.

3.5. Emission Spectra Measurements

The room temperature, solid-state excitation/emission deconvoluted spectra of each compound are shown in Figure 7, and their respective values in Table 2. These crystalline solids have interesting luminescent properties, with slight differences in their spectra (see Figure 10). There are no important differences between the spectra of the ligands with respect to the complexes, so it is possible to infer that the metal centers are not contributing to the molecular orbitals involved in the luminescence response.

In general, each compound shows the maximum excitation peaks at approximately 365 nm (see Table 2). The blueshift of the complex spectra may be attributed to the chelating or bridging effects of the ligands, due to their isomeric effect over the metal centers. Moreover, the bonding interaction between donor atoms and the Cd(II) center are slightly larger, agreeing with the Cambridge Crystallographic Data Base [41], which means that the contribution of the Cd(II) ion is negligible, explaining the slight blue-shifted bands, and focusing mainly on π–π* type transitions and the practically negligible metal-ligand charge transfer (MLCT) or ligand-metal charge transfer (LMCT), according to previously reported Cd(II) frameworks [42]

The spectra of all the compounds show important differences with respect to their luminescent intensities, which could be a consequence of the planar effect between pyridyl and triazole rings in the solid state. The compound **L1** could be less coplanar than compound **L2**; this difference is reflected in each complex, where the torsion angles between the fragments are 46.8(7)° for **L1** and 42.8(5)° for **L2**. Another plausible explanation for this difference could be due to the difference between the transition dipole moments of both compounds, where compound **L2** is higher than **L1**, as a consequence of a greater coplanar effect in compound **L2**.

For complexes **1** and **2**, the differences in the intensities could be due to the presence of water molecules in the tetraaquo complex **1**, because water molecules quench the basal state S_0, changing the luminescent absorption energy into vibrational energy released by O–H vibration modes [43]. The amplified luminescent response in the Cd(II) compounds does not correspond to major contribution of the metal centers. Rather, it is a linear response according to the number of ligands that each compound contains. Compound **1** contains two ligand units, while compound **2** has more ligand units due to its polymeric constitution. At this moment, we are working in the computational studies of a series of coordination polymers using DFT methods. In this work, the topological studies are also included.

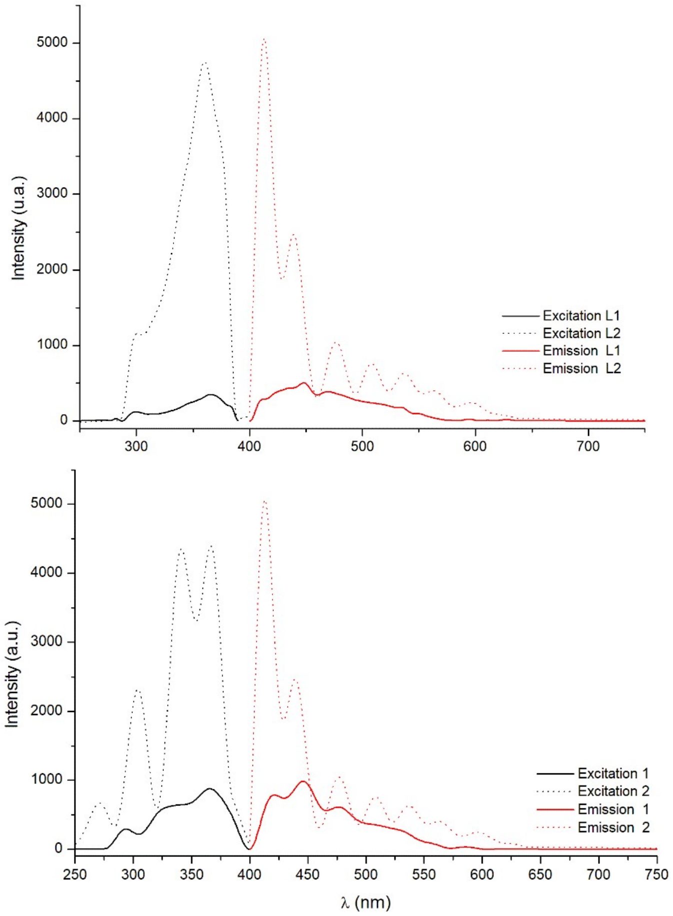

Figure 10. Deconvoluted excitation (black) and emission (red) spectra for compounds **L1** and **L2** (**top**) and compounds **1** and **2** (**bottom**).

Table 2. Excitation and emission data for compounds **L1**, **L2**, **1**, and **2**.

Compound	λ_{max} Excitation (nm)	λ_{max} Emission (nm)
L1	366	448
L2	360	413
1	366	446
2	366	412

4. Conclusions

We synthesized and characterized new types of Cd(II) complexes prepared via crystallization 2:1 with 5-methyl-1-(pyridin-3-yl)-1*H*-1,2,3-triazole-3-carboxylate (**L1**) and ethyl 5-methyl-1-(pyridin-3-yl)-1*H*-1,2,3-triazole-4-carboxylate (**L2**). The positional isomeric effect in compounds **L1** and **L2** gave rise to different types of Cd(II) compounds, a mononuclear discrete complex (**1**), and a Cd(II) framework, using **L2** as a linker between metal centers (**2**). Thermal analyses of compounds **1** and **2** reveal that both compounds are stable over 200 °C, being good candidates for the preparation of luminescent materials.

Supplementary Materials: The following are available online.

Author Contributions: J.C.; P.N., and C.A. performed the experiments; I.B., A.C., J.C., and J.L. wrote and edited the paper. I.B. got the founding acquisition for this research work.

Funding: This research was funded partially by Universidad de Antofagasta FONDECYT project 1170256

Acknowledgments: The authors thank Fondo de Desarrollo Nacional de Ciencia y Tecnología (FONDECYT) grant no.: 1170256, the Fondo Nacional de Equipamiento Científico (FONDEQUIP) grant no.: EQM 130021, and Vicerrectoría de Investigación de la Universidad de Antofagasta (VRI UA) J. Cisterna thanks the Universidad de Antofagasta for the postdoctoral fellowship.

Conflicts of Interest: The authors declare no conflict of interest.

References

1. Robin, A.Y.; Fromm, K.M. Coordination polymer networks with O- and N-donors: What they are, why and how they are made. *Coord. Chem. Rev.* **2006**, *250*, 2127–2157. [CrossRef]
2. Pettinari, C.; Tăbăcaru, A.; Galli, S. Coordination polymers and metal-organic frameworks based on poly(pyrazole)-containing ligands. *Coord. Chem. Rev.* **2016**, *307*, 1–31. [CrossRef]
3. Férey, G. Hybrid porous solids: Past, present, future. *Chem. Soc. Rev.* **2008**, *37*, 191–214. [CrossRef] [PubMed]
4. Almeida Paz, F.A.; Klinowski, J.; Vilela, S.M.F.; Tomé, J.P.C.; Cavaleiro, J.A.S.; Rocha, J. Ligand design for functional metal-organic frameworks. *Chem. Soc. Rev.* **2012**, *41*, 1088–1110. [CrossRef] [PubMed]
5. Bellussi, G.; Carati, A.; Rizzo, C.; Millini, R. New trends in the synthesis of crystalline microporous materials. *Catal. Sci. Technol.* **2013**, *3*, 833–857. [CrossRef]
6. Lalonde, M.; Bury, W.; Karagiaridi, O.; Brown, Z.; Hupp, J.T.; Farha, O.K. Transmetalation: Routes to metal exchange within metal-organic frameworks. *J. Mater. Chem. A* **2013**, *1*, 5453–5468. [CrossRef]
7. Falcaro, P.; Ricco, R.; Doherty, C.M.; Liang, K.; Hill, A.J.; Styles, M.J. MOF positioning technology and device fabrication. *Chem. Soc. Rev.* **2014**, *43*, 5513–5560. [CrossRef] [PubMed]
8. Czaja, A.U.; Trukhan, N.; Müller, U. Industrial applications of metal-organic frameworks. *Chem. Soc. Rev.* **2009**, *38*, 1284–1293. [CrossRef] [PubMed]
9. Allendorf, M.D.; Bauer, C.A.; Bhakta, R.K.; Houk, R.J.T. Luminescent metal-organic frameworks. *Chem. Soc. Rev.* **2009**, *38*, 1330–1352. [CrossRef] [PubMed]
10. Heine, J.; Müller-Buschbaum, K. Engineering metal-based luminescence in coordination polymers and metal–organic frameworks. *Chem. Soc. Rev.* **2013**, *42*, 9232. [CrossRef] [PubMed]
11. Cui, Y.; Yue, Y.; Qian, G.; Chen, B. Luminescent functional metal-organic frameworks. *Chem. Rev.* **2012**, *112*, 1126–1162. [CrossRef] [PubMed]
12. Binnemans, K. Lanthanide-Based Luminescent Hybrid Materials. *Chem. Rev.* **2009**, *109*, 4283–4374. [CrossRef] [PubMed]
13. Stavila, V.; Talin, A.A.; Allendorf, M.D. MOF-based electronic and opto-electronic devices. *Chem. Soc. Rev.* **2014**, *43*, 5994–6010. [CrossRef] [PubMed]
14. Yam, V.W.-W.; Lo, K.K.-W. Luminescent polynuclear d^{10} metal complexes. *Chem. Soc. Rev.* **1999**, *28*, 323–334. [CrossRef]
15. Huang, R.W.; Wei, Y.S.; Dong, X.Y.; Wu, X.H.; Du, C.X.; Zang, S.Q.; Mak, T.C. Hypersensitive dual-function luminescence switching of a silver-chalcogenolate cluster-based metal-organic framework. *Nat. Chem.* **2017**, *9*, 689–697. [CrossRef] [PubMed]
16. Wang, Z.; Su, H.F.; Tan, Y.Z.; Schein, S.; Lin, S.C.; Liu, W.; Wang, S.A.; Wang, W.G.; Tung, C.H.; Sun, D.; et al. Assembly of silver Trigons into a buckyball-like Ag_{180} nanocage. *Proc. Natl. Acad. Sci. USA* **2017**, *114*, 12132–12137. [CrossRef] [PubMed]
17. Liu, J.W.; Feng, L.; Su, H.F.; Wang, Z.; Zhao, Q.Q.; Wang, X.P.; Tung, C.H.; Sun, D.; Zheng, L.S. Anisotropic Assembly of Ag_{52} and Ag_{76} Nanoclusters. *J. Am. Chem. Soc.* **2018**, *140*, 1600–1603. [CrossRef] [PubMed]
18. Li, S.; Du, X.S.; Li, B.; Wang, J.Y.; Li, G.P.; Gao, G.G.; Zang, S.Q. Atom-Precise Modification of Silver(I) Thiolate Cluster by Shell Ligand Substitution: A New Approach to Generation of Cluster Functionality and Chirality. *J. Am. Chem. Soc.* **2018**, *140*, 594–597. [CrossRef] [PubMed]
19. Carlucci, L.; Ciani, G.; Proserpio, D.M. Polycatenation, polythreading and polyknotting in coordination network chemistry. *Coord. Chem. Rev.* **2003**, *246*, 247–289. [CrossRef]
20. Oshio, H.; Saito, Y.; Ito, T. Cluster Assembly by Hydrogen Bonds: Channel Structure of Cu4L4 Cubanes. *Angew. Chem. Int. Ed. Engl.* **1997**, *36*, 2673–2675. [CrossRef]
21. Du, M.; Bu, X.H.; Guo, Y.M.; Liu, H.; Batten, S.R.; Ribas, J.; Mak, T.C. First CuIIdiamondoid net with 2-fold interpenetrating frameworks. The role of anions in the construction of the supramolecular arrays. *Inorg. Chem.* **2002**, *41*, 4904–4908. [CrossRef] [PubMed]

22. Chatterjee, B.; Noveron, J.C.; Resendiz, M.J.E.; Liu, J.; Yamamoto, T.; Parker, D.; Cinke, M.; Nguyen, C.V.; Arif, A.M.; Stang, P.J. Self-assembly of flexible supramolecular metallacyclic ensembles: Structures and adsorption properties of their nanoporous crystalline frameworks. *J. Am. Chem. Soc.* **2004**, *126*, 10645–10656. [CrossRef] [PubMed]
23. Song, L.C.; Zhang, W.X.; Hu, Q.M. Syntheses and Characterizations of Novel One-dimensional Coordination Polymers Self-assembled from Co(NCS)2 and Flexible Diester-bridged Pyridine-based Ligands. *Chin. J. Chem.* **2010**, *20*, 1421–1429. [CrossRef]
24. Huang, F.P.; Tian, J.L.; Gu, W.; Liu, X.; Yan, S.P.; Liao, D.Z.; Cheng, P. Co(II) coordination polymers: Positional isomeric effect, structural and magnetic diversification. *Cryst. Growth Des.* **2010**, *10*, 1145–1154. [CrossRef]
25. Du, M.; Jiang, X.J.; Zhao, X.J. Molecular tectonics of mixed-ligand metal-organic frameworks: Positional isomeric effect, metal-directed assembly, and structural diversification. *Inorg. Chem.* **2007**, *46*, 3984–3995. [CrossRef] [PubMed]
26. Huang, F.P.; Tian, J.L.; Chen, G.J.; Li, D.D.; Gu, W.; Liu, X.; Yan, S.P.; Liao, D.Z.; Cheng, P. A case study of the ZnII-BDC/bpt mixed-ligand system: Positional isomeric effect, structural diversification and luminescent properties. *Cryst. Eng. Comm.* **2010**, *12*, 1269–1279. [CrossRef]
27. Liu, T.; Wang, S.; Lu, J.; Dou, J.; Niu, M.; Li, D.; Bai, J. Positional isomeric and substituent effect on the assemblies of a series of d^{10} coordination polymers based upon unsymmetric tricarboxylate acids and nitrogen-containing ligands. *Cryst. Eng. Comm.* **2013**, *15*, 5476–5489. [CrossRef]
28. Li, N.Y.; Ge, Y.; Wang, T.; Wang, S.J.; Ji, X.Y.; Liu, D. Construction of a series of coordination polymers based on 1,4-naphthalenedicarboxylic and flexible dipyridyl ligands. *Cryst. Eng. Comm.* **2014**, *16*, 2168. [CrossRef]
29. Bruker AXS Inc. *APEX3 Package. APEX3, SAINT and SADABS*; Bruker AXS Inc.: Madison, WI, USA, 2016.
30. Sheldrick, G.M. SHELXT—Integrated space-group and crystal-structure determination. *Acta Crystallogr. Sect. A Found. Crystallogr.* **2015**, *71*, 3–8. [CrossRef] [PubMed]
31. Sheldrick, G.M. Crystal structure refinement with SHELXL. *Acta Crystallogr. Sect. C Struct. Chem.* **2015**, *71*, 3–8. [CrossRef] [PubMed]
32. Spek, A.L. PLATON SQUEEZE: A tool for the calculation of the disordered solvent contribution to the calculated structure factors. *Acta Crystallogr. Sect. C Struct. Chem.* **2015**, *71*, 9–18. [CrossRef] [PubMed]
33. Dolomanov, O.V.; Bourhis, L.J.; Gildea, R.J.; Howard, J.A.K.; Puschmann, H. OLEX2: A complete structure solution, refinement and analysis program. *J. Appl. Crystallogr.* **2009**, *42*, 339–341. [CrossRef]
34. Brito, I.; Kesternich, V.; Pérez-Fehrmann, M.; Araneda, C.; Cárdenas, A. Crystal structure of ethyl 5-methyl-1-(pyridin-3-yl)-1H-1,2,3-triazole-4-carboxylate, $C_{11}H_{12}N_4O_2$. *Zeitschrift Für Krist—New Cryst. Struct.* **2017**, *232*, 1011–1012. [CrossRef]
35. Senthil, S.; Kamalraj, V.R.; Wu, S.L. Synthesis and characterization of ferroelectric liquid crystal dimers containing thioester and carboxylate linking groups in the inner side of the molecule. *J. Mol. Struct.* **2008**, *886*, 175–182. [CrossRef]
36. Allen, F.H.; Kennard, O.; Watson, D.G.; Brammer, L.; Orpen, A.G.; Taylor, R. Tables of Bond Lengths Determined by X-ray and Neutron-Diffraction. 1. Bond Lengths in Organic-Compounds. *J. Chem. Soc.; Perkin Trans 2.* **1987**, *12*, S1–S19. [CrossRef]
37. Cisterna, J.; Cárdenas, A.; Brito, I. Crystal structure of 4-aminopyridinium 4-acetyl-(pyridin-4-yl)-1*H*-1,2,3-triazol-5-olate monohydrate, $C_{14}H_{16}N_6O_3$. *Zeitschrift Für Krist—New Cryst. Struct.* **2018**, *233*, 571–573. [CrossRef]
38. Macksasitorn, S.; Hu, Y.; Stork, J.R. Homoconjugated 4-aminopyridine salts: Influence of anions on network topology. *Cryst. Eng. Comm.* **2013**, *15*, 1698–1705. [CrossRef]
39. Lu, M.; Wang, L.Y.; Hu, J.L.; Wang, Y.Y.; Yang, G.P. Syntheses, structures, and photoluminescence of a series of d^{10} coordination polymers with R-isophthalate (R. = -OH, $-CH_3$, and $-C.(CH_3)_3$). *Cryst. Growth Des.* **2009**, *9*, 5334–5342. [CrossRef]
40. Meng, G.X.; Feng, Y.M.; Wang, Y.; Gao, Y.L.; Wan, W.W.; Huang, X.T. Effect of pH on the self-assembly of three Cd(II) coordination compounds containing 5-(4-pyridyl)tetrazole: Syntheses, structures, and properties. *J. Coord. Chem.* **2015**, *68*, 1705–1718. [CrossRef]
41. Groom, C.R.; Bruno, I.J.; Lightfoot, M.P.; Ward, S.C. The Cambridge structural database. *Acta Crystallogr. Sect. B Struct. Sci. Cryst. Eng. Mater.* **2016**, *72*, 171–179. [CrossRef] [PubMed]

42. Wu, Y.; Yang, G.P.; Zhao, Y.; Wu, W.P.; Liu, B.; Wang, Y.Y. Three new solvent-directed Cd(ii)-based MOFs with unique luminescent properties and highly selective sensors for Cu^{2+}cations and nitrobenzene. *Dalt. Trans.* **2015**, *44*, 3271–3277. [CrossRef] [PubMed]
43. Dobretsov, G.E.; Syrejschikova, T.I.; Smolina, N.V. On mechanisms of fluorescence quenching by water. *Biophysics (Oxf)* **2014**, *59*, 183–188. [CrossRef]

Sample Availability: Samples of the compounds are available from the authors.